Supplementary Material: High-harmonic generation from spin-polarised defects in solids

Mrudul M. S. et al.

Supplementary Note 1: Direction resolved HHG-spectra

In Supplementary Fig. 1, we show the harmonics resolved in parallel and perpendicular configurations corresponding to the harmonics reported in Fig. 1a. The symmetry of the pristine h-BN permits the observation of the harmonics in the parallel and perpendicular configurations [1, 2]. Odd harmonics are present in the parallel configuration (see golden colour plot in Supplementary Fig. 1a), whereas even harmonics are present in the perpendicular configuration (see green colour plot in Supplementary Fig. 1b). For our specific laser polarisation, simple symmetry considerations imply that even harmonics should not be present in the parallel configuration, due to the presence of a mirror plane. Similar findings have been observed for MoS_2 in the experimental work by Liu et al. [2]. They attributed the presence of the harmonics in the perpendicular configuration to the anomalous intraband current, which arises from the Berry curvature of solids [2, 3]. In the case of V_B, we find that the observations made in the main text are applicable for both parallel and perpendicular configurations. There is an enhancement in the third harmonic as well as a decrease in the yield at higher energy compared to the HHG spectra of pristine h-BN.

Supplementary Note 2: Influence of electron-electron interaction in the electron dynamics

The total current calculated for pristine and V_B, in both the parallel and perpendicular configurations are compared in Supplementary Fig. 2 for TDDFT and IP models. Pristine h-BN shows a clear agreement for both parallel and perpendicular configurations. For V_B, the deviations from the IP model is more evident in the perpendicular configuration.

In Supplementary Fig. 3, we show the HHG spectrum of V_N to compare TDDFT and IP models.

Supplementary Note 3: Influence of defect-concentration

To check the influence of defect concentration, HHG is calculated for V_B in a 7×7 supercell. The 7×7 supercell is optimised with the methods specified in the main text. The ground-state is converged with a total magnetic moment of +1 μ_B. The Jahn-Teller distortion is observed again in this case. The defect gap-states are in good agreement with the

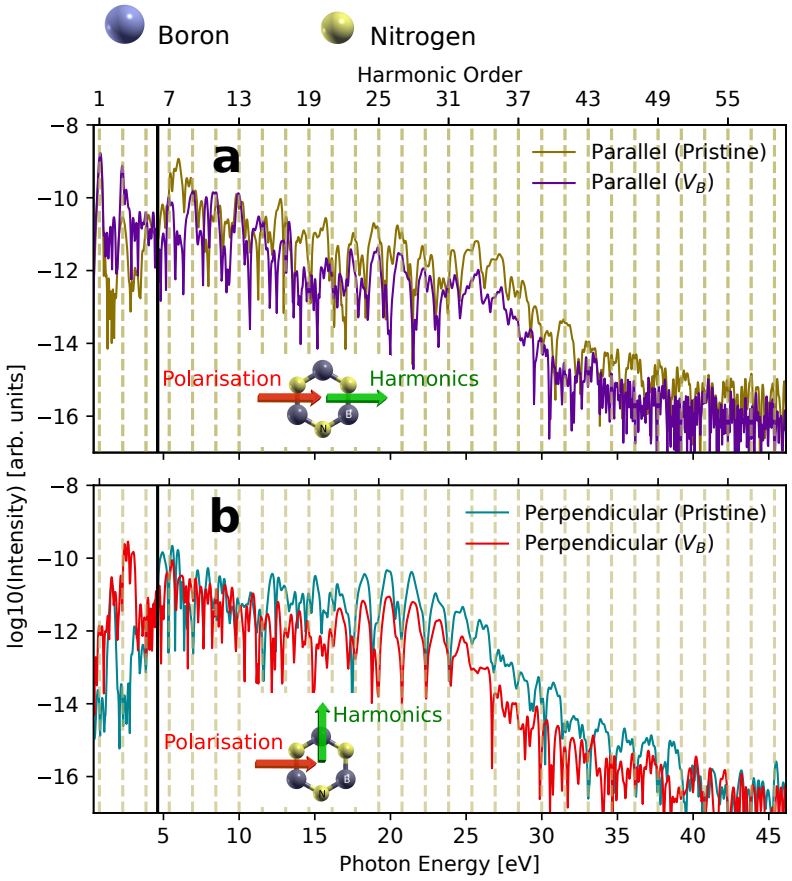

Supplementary Fig. 1. **Direction resolved high-order harmonic spectrum of monolayer hexagonal boron nitride (h-BN) with a boron vacancy**. **(a)** The parallel and **(b)** the perpendicular components of the total harmonic spectrum for V_B and pristine h-BN. The black vertical line presents the energy band-gap of h-BN. The parallel and perpendicular observational arrangements are shown in the inset. In parallel configuration, the laser polarisation (red arrow) is perpendicular to the boron-nitrogen bond, and the harmonics are observed along the same direction (green arrow), whereas the harmonics are observed perpendicular to the direction of laser polarisation in perpendicular configuration. Real-space geometric structure of h-BN is shown in which boron and nitrogen atoms are represented by grey and yellow colours, respectively.

5×5 supercell. The HHG spectra for V_B in a 7×7 supercell is compared with that of the pristine h-BN, as well as for V_B in a 5×5 supercell in Supplementary Fig 4.

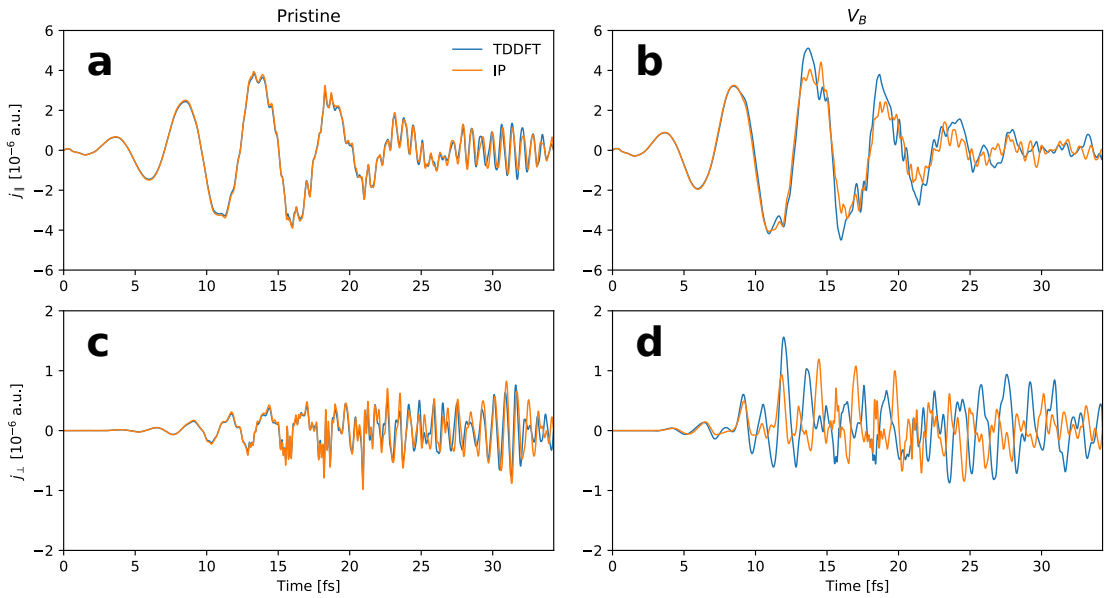

Supplementary Fig. 2. **Many-body effect in time-dependent current**. Parallel component of the total time-dependent current calculated using TDDFT (blue colour) and independent particle (IP) approximation (orange colour) for **(a)** pristine h-BN and **(b)** boron-vacant h-BN (V_B). The perpendicular component of the total time-dependent current for **(c)** pristine h-BN and **(d)** V_B.

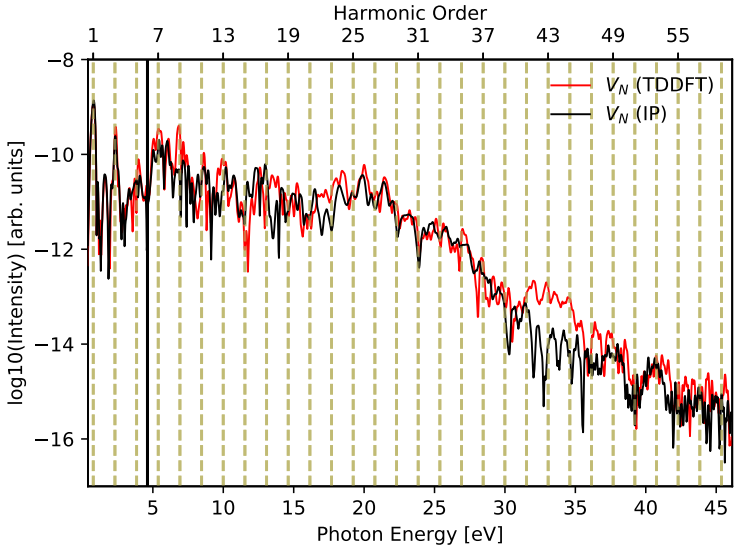

Supplementary Fig. 3. **Role of electron-electron interaction in the harmonic spectrum of V_N**. The harmonic spectrum within TDDFT and IP approximation are compared for nitrogen-vacant h-BN (V_N). The black vertical line presents the energy band-gap of pristine h-BN.

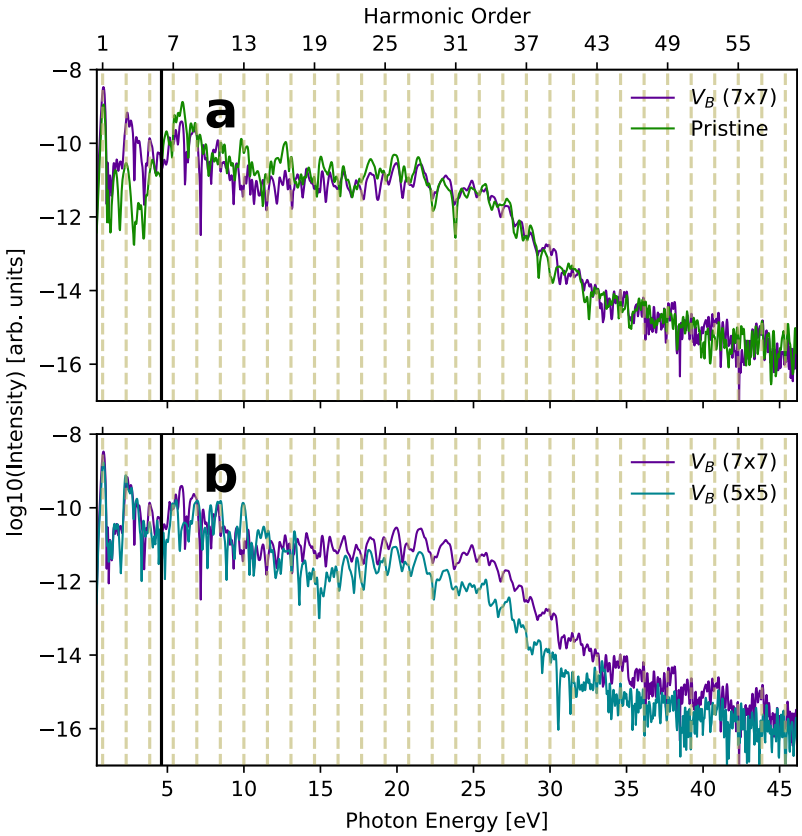

Supplementary Fig. 4. **Effect of defect concentration**. Total harmonic spectrum of h-BN with a boron-vacancy in a 7×7 supercell is compared with the harmonic spectrum of **(a)** pristine h-BN and **(b)** h-BN with a boron-vacancy in a 5×5 supercell. The black vertical line presents the energy band-gap of pristine h-BN.

Supplementary Note 4: Spin-resolved HHG-spectrum of V_N

In Supplementary Fig. 5, we report the complete spin-resolved harmonic spectra of V_N. The two spin-channels deviate slightly throughout the spectrum. The below band-gap part is shown in Fig. 5d.

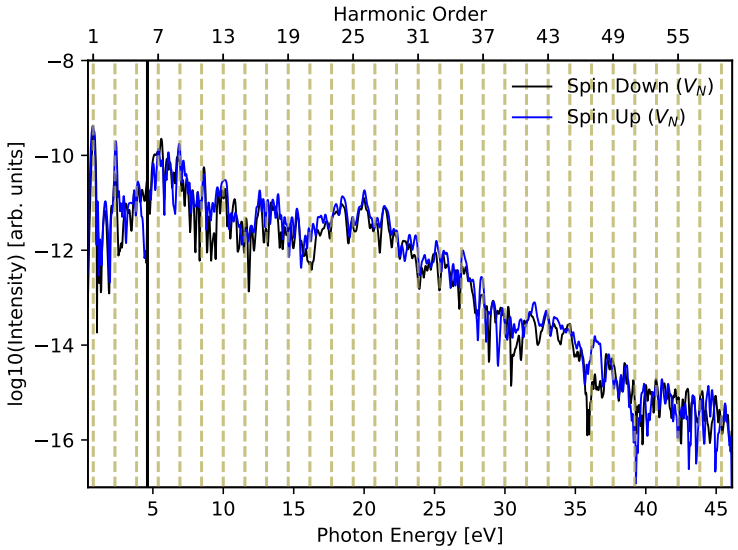

Supplementary Fig. 5. **Spin-resolved harmonic spectrum of V_N.** The spin-resolved total harmonic spectrum for h-BN with nitrogen vacancy (V_N). The black vertical line presents the energy band-gap of pristine h-BN.

Supplementary References

[1] G. Le Breton, A. Rubio, and N. Tancogne-Dejean. High-harmonic generation from few-layer hexagonal boron nitride: Evolution from monolayer to bulk response. *Physical Review B*, **98**(16): 165308 (2018).

[2] H. Liu, Y. Li, Y. S. You, S. Ghimire, T. F. Heinz, and D. A. Reis. High-harmonic generation from an atomically thin semiconductor. *Nature Physics*, **13**(3): 262 (2017).

[3] R. E. F. Silva, . Jimnez-Galn, B. Amorim, O. Smirnova, and M. Ivanov. All optical ultrafast probe of a topological phase transition. arXiv preprint arXiv:1806.11232, (2018).